Preparation and Characterization of 1−2 nm Dendrimer-Encapsulated Gold Nanoparticles Having Very Narrow Size Distributions

ARTICLE *in* CHEMISTRY OF MATERIALS · DECEMBER 2003

Impact Factor: 8.35 · DOI: 10.1021/cm034932o

3 AUTHORS, INCLUDING:

Sang-Keun Oh
TOPNANOSYS, Inc.
18 PUBLICATIONS **1,827** CITATIONS

SEE PROFILE

Preparation and Characterization of 1−2 nm Dendrimer-Encapsulated Gold Nanoparticles Having Very Narrow Size Distributions

Yong-Gu Kim, Sang-Keun Oh, and Richard M. Crooks*

Department of Chemistry, Texas A&M University, P.O. Box 30012, College Station, Texas 77842-3012

Received September 29, 2003

Highly monodisperse, 1−2-nm diameter Au nanoparticles were prepared using poly(amidoamine) (PAMAM) dendrimers as templates. The synthesis is carried out in water, takes less than 30 min, and requires no subsequent purification. Au nanoparticles having diameters of 1.3 ± 0.3 and 1.6 ± 0.3 nm were obtained when 55 and 140 equiv, respectively, of $HAuCl_4$ per dendrimer were used. For unpurified Au nanoparticles in this size range, this represents more than a 200% improvement in size distribution compared to previous reports. The high monodispersity is a function of the template synthesis, which avoids size variations arising from random nucleation and growth phenomena, and the use of magic number equivalent ratios of $AuCl_4^-$/dendrimer. When a nonmagic number of $AuCl_4^-$ equivalents per dendrimer was used, a significantly more polydisperse distribution of Au nanoparticles was obtained.

Introduction

We report the synthesis of nearly size-monodisperse Au nanoparticles prepared using a dendrimer templating approach.[1−7] Specifically, Au dendrimer-encapsulated nanoparticles (DENs) containing an average of 55 and 140 atoms and having sizes and size distributions of 1.3 ± 0.3 and 1.6 ± 0.3 nm, respectively, have been prepared within surface-functionalized poly(amidoamine) (PAMAM) dendrimers. For unpurified Au nanoparticles in this size range, this represents more than a 200% improvement compared to previously reported synthetic approaches where size distributions are reported.[7−9] Moreover, the nanoparticle synthesis is performed within a single aqueous phase and there are no variables in the synthesis that require careful control or that are difficult to reproduce.

Metal nanoparticles <4 nm in diameter are interesting because of their inherent size-dependent optical, electrical, catalytic, and magnetic properties.[10−15] These materials have been integrated into new kinds of biosensors,[16] used to study the effects of particle size on heterogeneous catalytic reactions,[15,17] and used to fabricate nanometer-scale electronic devices, such as single-electron transistors,[18] supercapacitors,[19] and data storage devices.[20] Further development in these fields awaits better synthetic approaches for preparing nanomaterials. Here, "better" means simpler syntheses that require minimal subsequent purification steps, more uniform particles having controllable architectures, higher levels of particle stability, particles having at least partially exposed surfaces, and simple linking chemistries that allow the particles to be attached to surfaces, polymers, and biomaterials without altering their physical and chemical properties.

A number of synthetic approaches have been used to improve the quality and control the physical properties of metal nanoparticles. These include stabilization of

* To whom correspondence should be addressed. E-mail: crooks@tamu.edu. Tel.: 979-845-5629. Fax: 979-845-1399.

(1) Zhao, M.; Sun, L.; Crooks, R. M. *J. Am. Chem. Soc.* **1998**, *120*, 4877−4878.
(2) Crooks, R. M.; Zhao, M.; Sun, L.; Chechik, V.; Yeung, L. K. *Acc. Chem. Res.* **2001**, *34*, 181−190.
(3) Crooks, R. M.; Lemon, B. I.; Sun, L.; Yeung, L. K.; Zhao, M. *Top. Curr. Chem.* **2000**, *212*, 81−135.
(4) Esumi, K.; Kameo, A.; Suzuki, A.; Torigoe, K. *Colloids Surf., A* **2001**, *189*, 155−161.
(5) Gröhn, F.; Bauer, B. J.; Akpalu, Y. A.; Jackson, C. L.; Amis, E. J. *Macromolecules* **2000**, *33*, 6042−6050.
(6) Zheng, J.; Petty, J. T.; Dickson, R. M. *J. Am. Chem. Soc.* **2003**, *125*, 7780−7781.
(7) Michels, J. J.; Huskens, J.; Reinhoudt, D. N. *J. Chem. Soc., Perkin Trans. 2* **2002**, 102−105.
(8) Hicks, J. F.; Templeton, A. C.; Chen, S.; Sheran, K. M.; Jasti, R.; Murray, R. W.; Debord, J.; Schaaf, T. G.; Whetten, R. L. *Anal. Chem.* **1999**, *71*, 3703−3711.
(9) Whetten, R. L.; Khoury, J. T.; Alvarez, M. M.; Murthy, S.; Vezmar, I.; Wang, Z. L.; Stephens, P. W.; Cleveland, C. L.; Luedtke, W. D.; Landman, U. *Adv. Mater.* **1996**, *8*, 428−433.
(10) Suzdalev, I. P.; Suzdalev, P. I. *Russ. Chem. Rev.* **2001**, *70*, 177−210.
(11) Rao, C. N. R.; Kulkarni, G. U.; Thomas, P. J.; Edwards, P. P. *Chem.-Eur. J.* **2002**, *8*, 29−35.
(12) Quinn, B. M.; Liljeroth, P.; Ruiz, V.; Laaksonen, T.; Kontturi, K. *J. Am. Chem. Soc.* **2003**, *125*, 6644−6645.
(13) Chen, S.; Ingram, R. S.; Hostetler, M. J.; Pietron, J. J.; Murray, R. W.; Schaaff, T. G.; Khoury, J. T.; Alvarez, M. M.; Whetten, R. L. *Science* **1998**, *280*, 2098−2101.
(14) Alvarez, M. M.; Khoury, J. T.; Schaaff, T. G.; Shafigullin, M. N.; Vezmar, I.; Whetten, R. L. *J. Phys. Chem. B* **1997**, *101*, 3706−3712.
(15) Valden, M.; Lai, X.; Goodman, D. W. *Science* **1998**, *281*, 1647−1650.
(16) Wang, J.; Xu, D.; Kawde, A.-N.; Polsky, R. *Anal. Chem.* **2001**, *73*, 5576−5581.
(17) Li, Y.; Boone, E.; El-Sayed, M. A. *Langmuir* **2002**, *18*, 4921−4925.
(18) Kastner, M. A. *Rev. Mod. Phys.* **1992**, *64*, 849−858.
(19) Kötz, R.; Carlen, M. *Electrochim. Acta* **2000**, *45*, 2483−2498.
(20) Jensen, T. R.; Malinsky, M. D.; Haynes, C. L.; Van Duyne, R. P. *J. Phys. Chem. B* **2000**, *104*, 10549−10556.

10.1021/cm034932o CCC: $27.50
Published on Web 12/06/2003

nanoparticles with micelles,[21] polymers,[22] and organic ligands.[23,24] For example, Boyen and co-workers prepared stabilized Au nanoparticles in the 1−8-nm size range using block copolymers and showed they self-assembled onto a variety of substrates.[25,26] Nanoparticles protected by organic ligands are particularly stable,[24] so quite a bit of effort has been focused on these materials. A major step forward in this regard is the phase-transfer synthetic approach for preparing monolayer-protected clusters (MPCs) first described by Brust,[27] and subsequently exploited by others for a variety of applications and fundamental studies.[8,9,28,29] MPCs typically have sizes ranging from 1.1 to 3.5 nm.[9,30] The size monodispersity is typically about ±1.0 nm, but it can be greatly improved by repeated fractional crystallization,[29] extraction and annealing,[12,31] or chromatography[29,32] into the range of ±0.2 to ±0.3 nm.

Dendrimers are good candidates for preparing metal nanoparticles because they can act as structurally and chemically well-defined templates and robust stabilizers. In addition, encapsulated nanoparticle surfaces are accessible to substrates so that catalytic reactions can be carried out.[33] Moreover, the solubility and reactivity of DENs can be controlled by appropriate functionalization of the peripheral groups. We and others have previously shown that metallic (Cu,[1] Pd,[34,35] Pt,[34,36,37] and Au[5,38]), bimetallic (Pd−Pt),[39] and semiconductor (CdS)[40] nanoparticles can be prepared within dendrimers. A typical synthesis is carried out by first sequestering metal ions within the dendrimer and then chemically reducing the resulting inorganic/organic nanocomposite.[2,3] In most cases, hydroxyl-terminated PAMAM dendrimers (G*n*-OH, where *n* represents the generation of the dendrimer) are used for this purpose because dendrimers having metal-complexing ligands, such as amine groups, on their periphery usually (but not always)[41] cross-link and precipitate in the presence of metal ions such as Cu, Pd, and Pt.[42,43] However, the synthesis of Au DENs within G*n*-OH dendrimers is complicated by the fact that the Au precursor complex ($HAuCl_4$) can be prematurely reduced by the peripheral hydroxyl groups.[38,44] This results in the formation of large Au particles that are not encapsulated within a single dendrimer.

Scheme 1

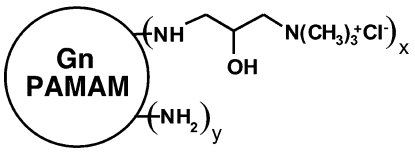

G4-Q_{32} : n = 4, x = 32, y = 32
G6-Q_{116} : n = 6, x = 116, y = 140

Dendrimers having functional groups on their surfaces other than hydroxyl groups have been used to prepare Au nanoparticles. Esumi et al. studied the formation of Au nanoparticles within PAMAM dendrimers carrying amine,[45] sugar,[44] methyl ester,[4] and alkyl groups[46] on their periphery. However, relatively large particles (2.1−12.8 nm) typically having broad size distributions were formed both in the interior and on the dendrimer exterior. Amis et al. reported the synthesis of Au nanoparticles synthesized using amine-terminated PAMAM dendrimers (G*n*-NH_2).[5,47] They prepared relatively large Au nanoparticles (2.0−4.0 nm) using G2−G10 dendrimers, but the size distributions determined by TEM were not clearly defined.[5] In addition, they reported that larger nanoparticles (4 nm) were obtained with G2 dendrimers than nanoparticles prepared in the presence of higher generations. This result indicates that low-generation dendrimers act exclusively as surface stabilizers, similar to the *n*-alkanethiols used to prepare MPCs.

Recently, we described PAMAM dendrimers having both quaternary ammonium groups and primary amines on their periphery (G*n*-Q_p, where *p* represents the number of quaternized peripheral groups) (Scheme 1).[48] We chose to use G*n*-Q_p dendrimers as templates in this work for two reasons. First, G*n*-Q_p dendrimers provide a synthetic handle (specifically, the unfunctionalized primary amines) for subsequent covalent attachment of the Au DENs to surfaces and other molecules. Second, the quaternized amines provide a large positive charge on the dendrimer periphery and thereby reduce the likelihood of DEN agglomeration. For example, we previously showed that highly monodisperse Pd and Pt

(21) Veisz, B.; Király, Z. *Langmuir* **2003**, *19*, 4817−4824.
(22) Walker, C. H.; St John, J. V.; Wisian-Neilson, P. *J. Am. Chem. Soc.* **2001**, *123*, 3846−3847.
(23) Wang, Y. A.; Li, J. J.; Chen, H.; Peng, X. *J. Am. Chem. Soc.* **2002**, *124*, 2293−2298.
(24) Templeton, A. C.; Wuelfing, W. P.; Murray, R. W. *Acc. Chem. Res.* **2000**, *33*, 27−36.
(25) Boyen, H.-G.; Kästle, G.; Weigl, F.; Koslowski, B.; Dietrich, C.; Ziemann, P.; Spatz, J. P.; Riethmüller, S.; Hartmann, C.; Möller, M.; Schmid, G.; Garnier, M. G.; Oelhafen, P. *Science* **2002**, *297*, 1533−1536.
(26) Spatz, J. P.; Mössmer, S.; Hartmann, C.; Möller, M.; Herzog, T.; Krieger, M.; Boyen, H.-G.; Ziemann, P.; Kabius, B. *Langmuir* **2000**, *16*, 407−415.
(27) Brust, M.; Walker M.; Bethell, D.; Schiffrin, D. J.; Whyman, R. *J. Chem. Soc., Chem. Commun.* **1994**, 801−803.
(28) Chen, S.; Pei, R. *J. Am. Chem. Soc.* **2001**, *123*, 10607−10615.
(29) Schaaff, T. G.; Shafigullin, M. N.; Khoury, J. T.; Vezmar, I.; Whetten, R. L.; Cullen, W. G.; First, P. N.; Gutiérrez-Wing, C.; Ascensio, J.; Jose-Yacamán, M. J. *J. Phys. Chem. B* **1997**, *101*, 7885−7891.
(30) Lee, D.; Donkers, R. L.; DeSimone, J. M.; Murray, R. W. *J. Am. Chem. Soc.* **2003**, *125*, 1182−1183.
(31) Hicks, J. F.; Miles, D. T.; Murray, R. W. *J. Am. Chem. Soc.* **2002**, *124*, 13322−13328.
(32) Jimenez, V. L.; Leopold, M. C.; Mazzitelli, C.; Jorgenson, J. W.; Murray, R. W. *Anal. Chem.* **2003**, *75*, 199−206.
(33) Niu, Y.; Yeung, L. K.; Crooks, R. M. *J. Am. Chem. Soc.* **2001**, *123*, 6840−6846.
(34) Zhao, M.; Crooks, R. M. *Angew. Chem., Int. Ed.* **1999**, *38*, 364−366.
(35) Ooe, M.; Murata, M.; Mizugaki, T.; Ebitani, K.; Kaneda, K. *Nano Lett.* **2002**, *2*, 999−1002.
(36) Zhao, M.; Crooks, R. M. *Adv. Mater.* **1999**, *11*, 217−220.
(37) Esumi, K.; Nakamura, R.; Suzuki, A.; Torigoe, K.*Langmuir* **2000**, *16*, 7842−7846.
(38) West, R.; Wang, Y.; Goodson, T. *J. Phys. Chem. B* **2003**, *107*, 3419−3426.
(39) Scott, R. W. J.; Datye, A. K.; Crooks, R. M. *J. Am. Chem. Soc.* **2003**, *125*, 3708−3709.
(40) Lemon, B. I.; Crooks, R. M. *J. Am. Chem. Soc.* **2000**, *122*, 12886−12887.
(41) Ye, H.; Scott, R. W. J.; Crooks, R. M. **2003**, submitted for publication.
(42) Garcia, M. E.; Baker, L. A.; Crooks, R. M. *Anal. Chem.* **1999**, *71*, 256−258.
(43) Esumi, K.; Suzuki, A.; Yamahira, A.; Torigoe, K. *Langmuir* **2000**, *16*, 2604−2608.
(44) Esumi, K.; Hosoya, T.; Suzuki, A.; Torigoe, K. *Langmuir* **2000**, *16*, 2978−2980.
(45) Esumi, K.; Torigoe, K. *Prog. Colloid. Polym. Sci.* **2001**, *117*, 80−87.
(46) Esumi, K.; Hosoya, T.; Suzuki, A.; Torigoe, K. *J. Colloid Interface Sci.* **2000**, *229*, 303−306.
(47) Gröhn, F.; Kim, G.; Bauer, B. J.; Amis, E. J. *Macromolecules* **2001**, *34*, 2179−2185.
(48) Oh, S.-K.; Kim, Y.-G.; Ye, H.; Crooks, R. M. *Langmuir* **2003**, *19*, 10420−10425.

nanoparticles could be prepared within G*n*-Q_p dendrimers and that the resulting composites could be covalently linked to a self-assembled monolayer (SAM).[48,49]

Experimental Section

Chemicals. Partially quaternized fourth- and sixth-generation dendrimers (G4-Q_{32} and G6-Q_{116}) were synthesized from fourth- and sixth-generation amine-terminated PAMAM dendrimers (G4-NH_2 and G6-NH_2) as previously reported.[48] G4-NH_2 and G6-NH_2 in methanol were obtained from Dendritech, Inc. (Midland, MI) and dried under vacuum to remove the solvent prior to use. $HAuCl_4$ and $NaBH_4$ were purchased from the Aldrich Chemical Co. (Milwaukee, WI) and used as received. NaOH was purchased from the EM science (Gibbstown, NJ) and 18 MΩ·cm Milli-Q water (Millipore, Bedford, MA) was used throughout.

DEN Synthesis. A 10 μM G*n*-Q_p aqueous solution (0.5 mL) and 55, 100, 140, or 300 equiv of 2 mM $HAuCl_4$ in water were mixed. This pale yellow solution was vigorously stirred for 20 min to provide enough time for $HAuCl_4$ to be extracted into the dendrimer interior. A 5-fold molar excess of $NaBH_4$ in 0.3 M NaOH was quickly added to this solution with stirring to reduce the Au complex to zerovalent Au, and immediately the color changed from yellow to brown. $NaBH_4$ was dissolved in 0.3 M NaOH, which helps to decrease the rate of reduction.[5] Following the synthesis, the total solution volume was 5 mL and the final concentration of DENs was 1 μM. G4-NH_2 dendrimers were also used to prepare Au DENs (G4-NH_2-(Au_{55})) using the same method described for the synthesis of G4-Q_{32}(Au_{55}). All DENs were characterized without being purified.

Characterization. UV−vis absorbance spectra were obtained using quartz cells and a Hewlett-Packard 8453 UV−vis spectrometer system (Hewlett-Packard, Wilmington, DE) at 25 ± 2 °C. UV−vis spectra were obtained using 1 μM G6-Q_{116} and 140 μM $HAuCl_4$ aqueous solutions or 0.5 μM aqueous Au DEN solutions. High-resolution transmission electron microscopy (HRTEM) was performed using a JEOL 2010 electron microscope (JEOL USA Inc., Peabody, MA). Samples were prepared by placing 3 drops of 1 μM aqueous Au DEN solutions on carbon-coated copper grids (EM science, Gibbstown, NJ) and allowing the solvent to evaporate in air.

Results and Discussion

Preparation of Au DENs. Au nanoparticles were prepared within fourth- and sixth-generation PAMAM dendrimers having about 50% of their peripheral amine groups modified with ammonium chloride (G4-Q_{32} and G6-Q_{116}, respectively, Scheme 1).[48] Because they are quaternized, G*n*-Q_p dendrimers have permanent positive charges at their periphery. This high charge density minimizes the likelihood of dendrimer aggregation[5] and of multiple dendrimers stabilizing a single nanoparticle,[4,42] and it therefore enhances the probability of intradendrimer nanoparticle formation. Encapsulated Au nanoparticles were synthesized within quaternized dendrimers using a two-step process: extraction of aqueous $AuCl_4^-$ into the dendrimer interior, followed by reduction with $NaBH_4$ in 0.3 M NaOH solution.[5] Specifically, $HAuCl_4$ (55, 100, 140, or 300 equiv per dendrimer) was mixed with 0.5 mL of an aqueous 10 μM G*n*-Q_p aqueous solution. This pale yellow solution was vigorously stirred for 20 min to provide enough time for $HAuCl_4$ to be extracted into the dendrimer interior. Second, a 5-fold molar excess of $NaBH_4$ in 0.3 M NaOH was quickly added to this solution with stirring to reduce the Au complex to zerovalent Au. This resulted in conversion of the initially pale yellow solution to the characteristic brown color of Au nanoparticles (<2 nm).

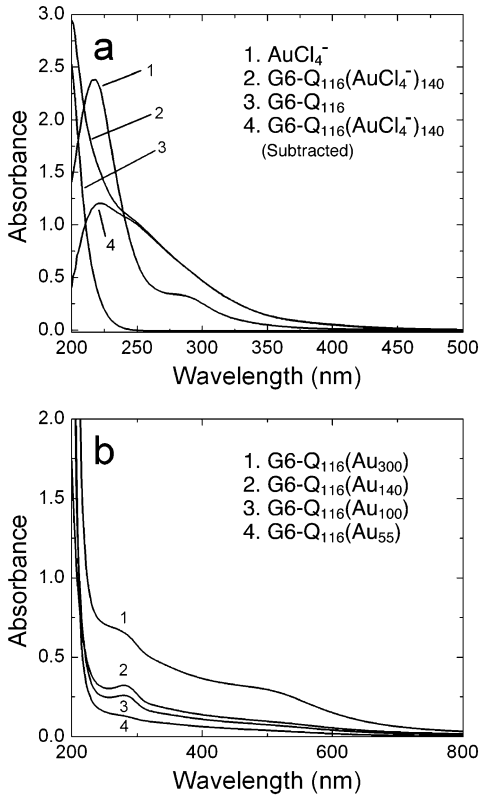

Figure 1. (a) UV−vis spectra of aqueous solutions of (1) $AuCl_4^-$, (2) G6-Q_{116}($AuCl_4^-$)$_{140}$, and (3) G6-Q_{116} obtained using H_2O as a background spectrum. For comparison, spectrum 4 was obtained by subtracting spectrum 3 from spectrum 2. The spectra were obtained using solutions containing 1.0 μM G6-Q_{116} and 140 μM $AuCl_4^-$. (b) UV−vis spectra of aqueous solutions containing (1) G6-Q_{116}(Au_{300}), (2) G6-Q_{116}(Au_{140}), (3) G6-Q_{116}(Au_{100}), and (4) G6-Q_{116}(Au_{55}). The spectra were obtained from 0.5 μM Au DEN solutions.

UV−Vis Absorbance Spectroscopy. Figure 1a shows UV−vis absorbance spectra of aqueous solutions containing $AuCl_4^-$, G6-Q_{116}, and G6-Q_{116}($AuCl_4^-$)$_{140}$ before reduction with $NaBH_4$. The UV−vis spectrum of $AuCl_4^-$ reveals a strong absorption band at 220 nm and a shoulder at 290 nm. These bands were previously assigned as ligand-to-metal-charge-transfer (LMCT) transitions.[43] The spectrum of G6-Q_{116} is featureless, except for a rapidly increasing absorbance below about 230 nm. When G6-Q_{116} and $AuCl_4^-$ are mixed, the resulting spectrum, after subtraction of the G6-Q_{116} background, is different from the spectrum of a solution containing only $AuCl_4^-$. Specifically, the intensity of the band at 220 nm decreases and shifts to lower energy by 5 nm, while the intensity of the shoulder at 290 nm increases and broadens. The broad band centered around 290 nm is characteristic of ion-pair formation between $AuCl_4^-$ and G6-Q_{116}.[43]

Absorbance spectroscopy is useful for studying metal nanoparticles because the peak positions and shapes are sensitive to particle size. For example, Au nanoparticles larger than 2 nm typically have a plasmon band in the range of 500−550 nm.[11,14] However, when the particle size is less than 2 nm, the distinctive plasmon band is

(49) Scott, R. W. J.; Ye, H.; Henriquez, R. R.; Crooks, R. M. *Chem. Mater.* **2003**, *15*, 3873−3878.

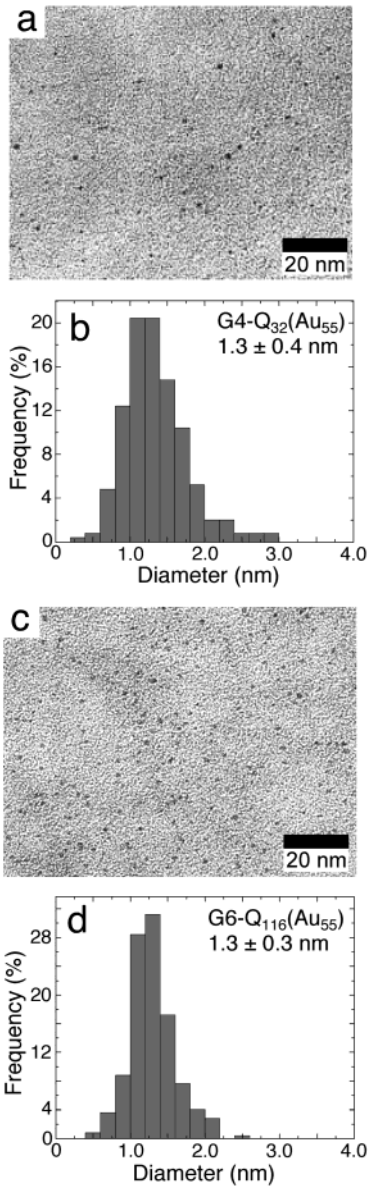

Figure 2. HRTEM images of (a) G4-Q_{32}(Au_{55}) and (c) G6-Q_{116}-(Au_{55}) and corresponding particle size distributions (b and d, respectively). The average Au particle diameters are 1.3 ± 0.4 nm for G4-Q_{32}(Au_{55}) and 1.3 ± 0.3 nm for G6-Q_{116}(Au_{55}).

replaced by a featureless absorbance, which increases monotonically toward higher energies.[6,50] This behavior is apparent in Figure 1b. There is no plasmon band apparent in spectra 2−4, which correspond to Au DENs containing an average of 140, 100, and 55 atoms, respectively. This result suggests that these particles are less than 2 nm in diameter. When the [$HAuCl_4$]:[G6-Q_{116}] ratio increases to 300, however, a plasmon band appears as a broad and indistinct feature centered at 510 nm (Spectrum 1, Figure 1b).

High-Resolution Transmission Electron Microcopy. Figure 2 shows HRTEM images and size-distribution histograms for G4-Q_{32}(Au_{55}) and G6-Q_{116}-(Au_{55}). The images reveal widely separated Au nanoparticles and little aggregation. This may be a consequence of the high charge density on the surface of the quaternized host dendrimers. The average sizes of the

Table 1. Comparison between Calculated and Measured Diameters of Au DENs

DEN	calculated diameter[a] (nm)	measured diameter[b] (nm)
G4-Q_{32}(Au_{55})	1.2	1.3 ± 0.4
G6-Q_{116}(Au_{55})	1.2	1.3 ± 0.3
G4-Q_{32}(Au_{140})	1.6	1.6 ± 0.4
G6-Q_{116}(Au_{140})	1.6	1.6 ± 0.3
G6-Q_{116}(Au_{100})	1.4	1.4 ± 0.6

[a] Calculated using the equation: $n = 4\pi(R - \delta)^3/3\nu_g$, where n is the number of Au atoms, R is the radius of Au nanoparticle, δ is the length of the protecting ligands (in this case, $\delta = 0$), and ν_g is the volume of one Au atom (17 Å^3).[51] [b] Measured from HRTEM images.

G4-Q_{32}(Au_{55}) and G6-Q_{116}(Au_{55}) DENs are 1.3 ± 0.4 and 1.3 ± 0.3 nm, respectively. A few particles having diameters larger than 2 nm are also present, but we suspect these arise from two or more overlapping small particles that appear in the two-dimensional HRTEM projection as a single larger particle. Note that the average size of the Au_{55} nanoparticles measured by HRTEM is very close to the value of 1.2 nm calculated by assuming that these materials are spherical in shape (Table 1).[51]

Figure 3 shows HRTEM images of G4-Q_{32}(Au_{140}) and G6-Q_{116}(Au_{140}) and corresponding histograms of particle size distributions. The measured diameters of G4-Q_{32}-(Au_{140}) and G6-Q_{116}(Au_{140}) are 1.6 ± 0.4 and 1.6 ± 0.3 nm, respectively. As for the 55-atom DENs, these nanoparticles do not agglomerate and the average size (1.6 nm) is identical to the calculated value for particles containing this number of atoms. The measured diameters of Au nanoparticles from HRTEM images are compared to calculated values and summarized in Table 1.

An interesting conclusion that can be drawn from Figures 2 and 3 is that the size of the Au nanoparticles does not depend on the dendrimer generation, but rather only on the [$HAuCl_4$]:[Gn-Q_p] ratio. In contrast, it has previously been reported that for amine-terminated PAMAM dendrimers the size of Au nanoparticles decreases as the dendrimer generation increases.[42,43,45] Although not conclusively demonstrated, the contention was that multiple low-generation dendrimers stabilize each nanoparticle, whereas for higher generations, smaller Au nanoparticles are encapsulated within individual dendrimers. That is, in the former case the nanoparticles are stabilized by primary amine peripheral groups rather than by true encapsulation within single dendrimers. Therefore, the observed independence of nanoparticle size on the dendrimer generation here provides evidence that the nanoparticles are truly templated by the interior of individual dendrimers.

It is also interesting to note that 140-atom DENs can be formed within the interior of the G4-Q_{32} dendrimer, which only contains 62 internal tertiary amine groups. With one exception,[52] previous reports from us[2] and others[5,37] have shown that the number of metal atoms that can be contained within a dendrimer is approximately equal to or less than the number of interior tertiary amines. This is because metal ion encapsulation

(50) Roldughin, V. I. *Russ. Chem. Rev.* **2000**, *69*, 821−843.
(51) Leff, D. V.; Ohara, P. C.; Heath, J. R.; Gelbart, W. M. *J. Phys. Chem.* **1995**, *99*, 7036−7041.
(52) Niu, Y.; Crooks, R. M. *Chem. Mater.* **2003**, *15*, 3463−3467.

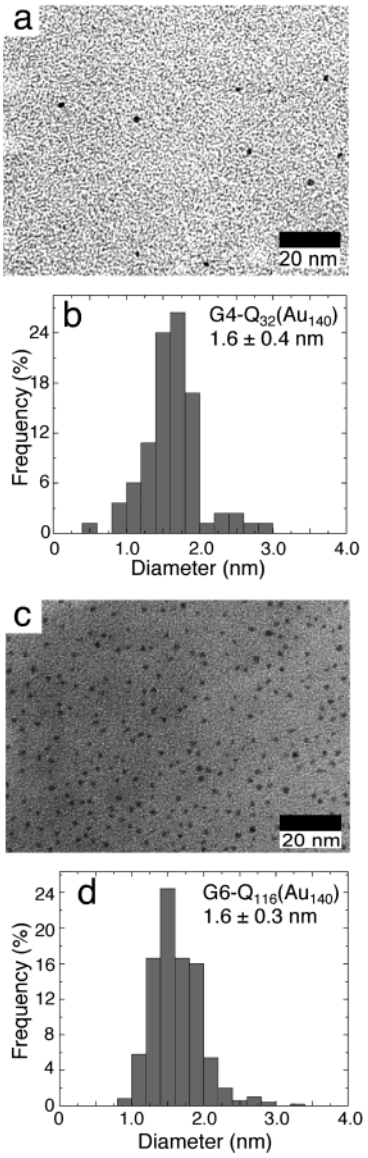

Figure 3. HRTEM images of (a) G4-Q_{32}(Au_{140}) and (c) G6-Q_{116}(Au_{140}) and corresponding particle size distributions (b and d, respectively). The average Au particle diameters are 1.6 ± 0.4 nm for G4-Q_{32}(Au_{140}) and 1.6 ± 0.3 nm for G6-Q_{116}(Au_{140}).

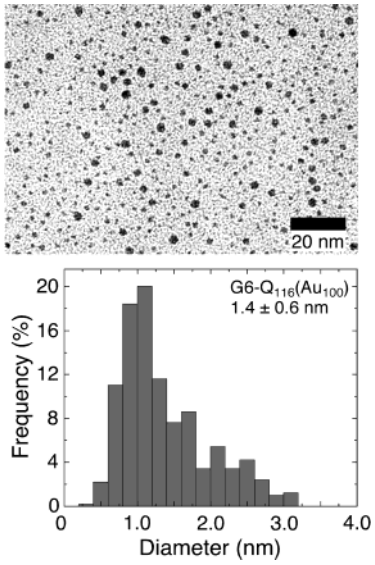

Figure 4. HRTEM image and corresponding particle size distribution for G6-Q_{116}(Au_{100}). The average Au particle diameter is 1.4 ± 0.6 nm.

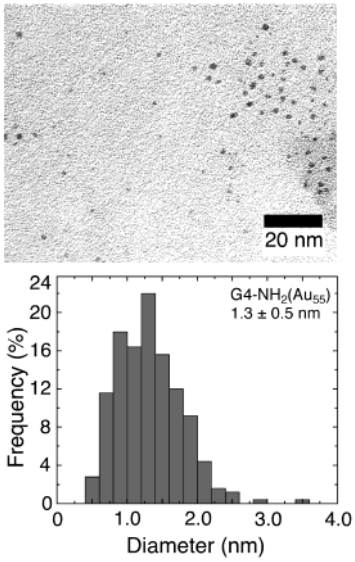

Figure 5. HRTEM image and corresponding particle size distribution for G4-NH_2(Au_{55}). The average Au particle diameter is 1.3 ± 0.5 nm.

of Cu, Pd, and Pt salts are driven by specific interactions with these interior functional groups. In the one exception to this general finding the metal ions were driven into the dendrimer interior by differences in the dielectric strength of the solvent and dendrimer interior.[52] Taken together, these findings may suggest that $AuCl_4^-$ encapsulation within G*n*-Q_p is driven by electrostatic interactions and perhaps also solubility differences of $AuCl_4^-$ in water compared to the dendrimer interior.[5,7] However, this is just speculation, and at the present time the driving force for $AuCl_4^-$ encapsulation is unknown.

The formation of the highly monodisperse Au nanoparticles reported here is possible in part because particular [$HAuCl_4$]:[G*n*-Q_p] ratios were used to prepare them. Metal nanoparticles containing these "magic numbers" of atoms form energetically favorable, closed-shell crystals.[24] To verify that magic numbers of metal atoms are important for high monodispersity, we prepared Au nanoparticles using an intermediate [$HAuCl_4$]:[G6-Q_{116}] ratio of 100. Figure 4 shows the results of a HRTEM study of G6-Q_{116}(Au_{100}). The important observation is that the particle size distribution appears somewhat bimodal, and it is therefore not as narrow as for G6-Q_{116}(Au_{55}) or G6-Q_{116}(Au_{140}). Specifically, the average particle size for G6-Q_{116}(Au_{100}) is 1.4 ± 0.6 nm compared to 1.3 ± 0.3 nm and 1.6 ± 0.3 nm for G6-Q_{116}(Au_{55}) and G6-Q_{116}(Au_{140}), respectively.

To better understand the impact of the partially quaternized surface of G4-Q_{32} on the properties of encapsulated Au nanoparticles, we compared the average Au particle size and size distribution for nanoparticles prepared using G4-NH_2 and G4-Q_{32} templates. In both cases an [$HAuCl_4$]:[dendrimer] ratio of 55 was used. A HRTEM image of Au nanoparticles prepared within G4-NH_2 (Figure 5) reveals a slightly broader size distribution (1.3 ± 0.5 nm) compared to that of G4-Q_{32}-(Au_{55}) (Figure 2a, 1.3 ± 0.4 nm). This result suggests that the main function of the quaternary amine groups is to prevent agglomeration of dendrimers, but that the

charged surface exerts only a slight influence over the size of the encapsulated nanoparticles. This result is consistent with the dendrimer interior, rather than the periphery, controlling the size and size distribution of the particles. It may also suggest that factors other than electrostatic interactions control $AuCl_4^-$ encapsulation.

Summary and Conclusions

The key result of this study is elucidation of a very simple, template-based approach for preparing size-monodisperse Au nanoparticles in the interesting size range of 1−2 nm. We believe the monodispersity of Au DENs prepared within G*n*-Q_p is enhanced by three factors. First, because this is a template-based approach, the variation of nanoparticle size that is inevitable for methods that rely on nucleation-and-growth phenomena is avoided. Second, the high permanent charge on the surface of the G*n*-Q_p dendrimers lessens the likelihood of aggregation. Third, we chose to use "magic number"[24,53] ratios of [$HAuCl_4$]:[G*n*-Q_p] because it has previously been shown that Au nanoparticles containing 55 or 140 atoms form energetically favorable structures.[9,54] When magic numbers of metal atoms were not used (e.g., [$HAuCl_4$]:[G*n*-Q_p] = 100), the formation of a significantly more polydisperse population of Au nanoparticles was observed.

Robust synthetic routes to monodisperse nanomaterials is an essential first step toward technologies that incorporate these materials, and there are some significant advantages of the approach described here for preparing Au nanoparticles. First, this approach is simple and highly reproducible and does not require careful control of experimental conditions. Second, a high level of monodispersity is attained without the need for subsequence purification. Third, as we have shown previously for Pd DENS,[33,34] the surface of the particles is accessible, and thus these materials can be used for catalysis. Fourth, the dendrimer itself provides a convenient means for linking DENs to other molecules or surfaces.[48] Finally, we have recently shown that both Pd and Au nanoparticles can be extracted from dendrimer templates with little or no change to their physical properties.[55] Our next step is to better understand the electronic and photonic properties of these materials,[31,56] and to further refine the synthesis with a view toward improving the size distribution to the resolution of available characterization methods, which seems to be limited to about ±0.15 nm.

Acknowledgment. This material is based in part upon work supported by the National Science Foundation under Grant No. 0211068. We also acknowledge the Robert A. Welch Foundation for financial support. We thank Dr. Robert W. J. Scott for helpful discussions. We also thank Dr. Zhiping Luo and E. Ann Ellis of the TAMU Microscopy and Imaging Center for their assistance.

CM034932O

(53) Mottet, C.; Tréglia, G.; Legrand, B. *Surf. Sci.* **1997**, *383*, L719−L727.
(54) Schmid, G. *Chem. Rev.* **1992**, *92*, 1709−1727.
(55) Garcia-Martinez, J. C.; Scott, R. W. J.; Crooks, R. M. *J. Am. Chem. Soc.* **2003**, *125*, 11190−11191.
(56) Hicks, J. F.; Zamborini, F. P.; Osisek, A. J.; Murray, R. W. *J. Am. Chem. Soc.* **2001**, *123*, 7048−7053.